Supplemental information for “Positron-Induced Luminescence”

E. V. Stenson, U. Hergenhahn, M. R. Stoneking, and T. Sunn Pedersen

(Dated: April 6, 2018)

Abstract

This document provides supplemental information for the article “Positron-Induced Luminescence”, including typical image data and beam energy distributions. It also gives some additional specifics of the luminescence measurements — i.e., the verification that luminescence increases linearly with current and the determination of the proportionality constant for this relationship. The conclusions of the above are summarized in the main manuscript, but further details are provided here, in case some readers may be interested in them. Additionally, we provide plots that calculate the differences and ratios between positron and electron luminescence, with uncertainties. These are derived from the data already showcased in the main manuscript, but in case readers may be interested in these derived quantities rather than the original curves, they are included as a reference.[a]

[a] This description is courtesy of PRL (©2018 American Physical Society) and is vastly superior to the one we originally supplied: “This document provides supplemental information for the manuscript ‘Positron-induced luminescence’, including figures and details of the methodology that are of value but likely of limited reader interest.” (EVS)

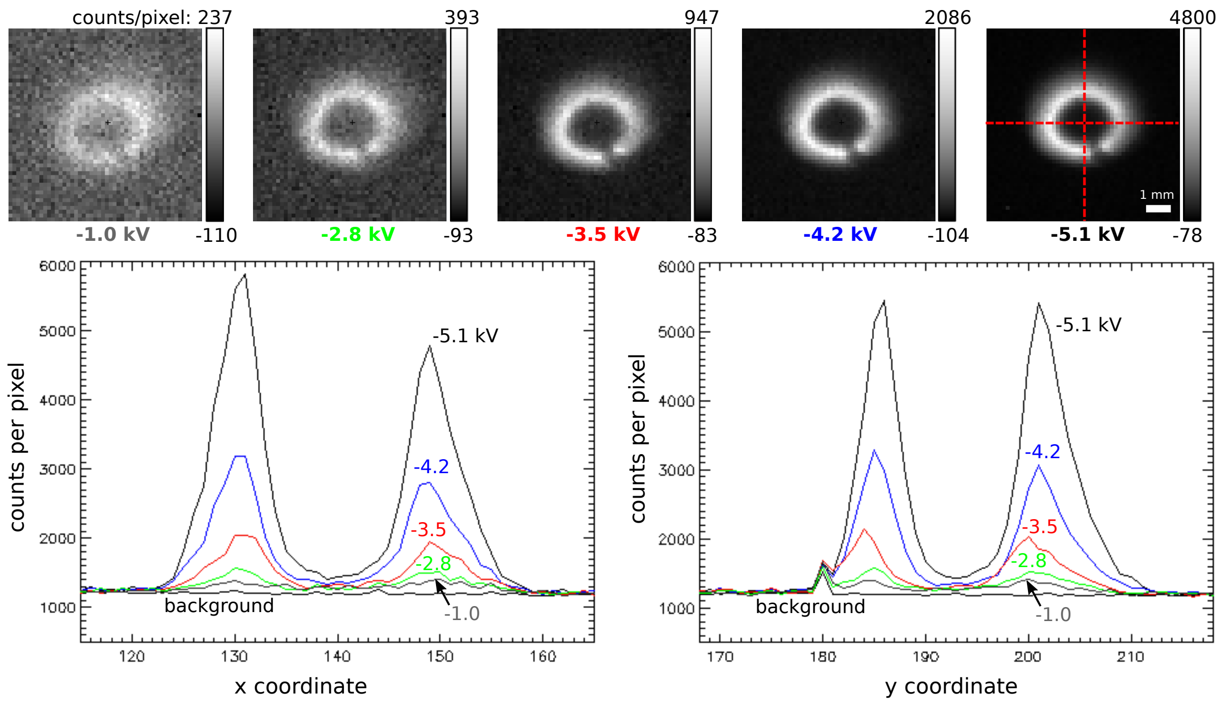

FIG. 1. Top row: 50x50 pixel counting window in background-subtracted images of the positron beam incident on the Zns:Ag screen, for five different values of the screen bias. Bottom row: Cross-sections through the center of the counting window (marked in the top right image with dashed red lines) for each of the five above images prior to background-subtraction, as well as for the background image.

Typical background-subtracted image data is shown in the top section of Fig. 1. Below are plots of cross-sections through these images prior to background subtraction. One point to note is that the excess positron luminescence — exemplified by the image at $V = -1.0$ kV — is highly localized at the location of the incident beam. If this additional luminescence were caused by scintillation of 511-keV annihilation gamma rays, for which the mean free path in materials is much larger than the thickness of the phosphor layer, the additional luminescncе would be expected to be distributed fairly evenly across the screen. Therefore, we conclude that no appreciable contribution from annihilation-gamma-induced scintillation is seen (as one might expect, given that scintillation detectors typically require single crystals that are several centimeters in linear dimension).

A typical energy distribution measurement for each species is shown in Fig. 2. The parallel temperature is on the order of some eV (2 eV for the electron beam, 6 eV for the positron beam); the perpendicular temperature is expected to be at most of the same order.

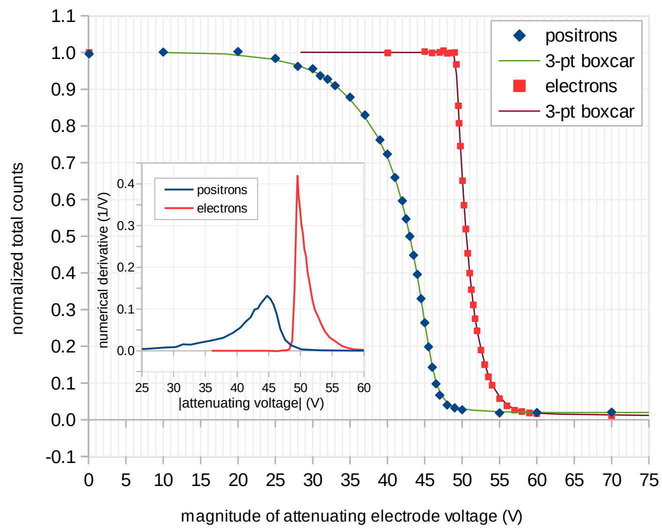

FIG. 2. The longitudinal energy and temperature of each beam (prior to acceleration onto the screen) are indicated by the dependence of phosphor screen luminescence on the magnitude of a retarding potential applied upstream (as shown in Fig. 2 in the main manuscript). Data have been normalized to the luminescence of the full beam for each species. Uncertainties are on the order of the symbol size. Lines show three-point boxcar averages, the numerical derivatives of which are shown in the inset.

Thus, both are small relative to the beam energy (especially after kV-scale acceleration onto the screen). As shown here, the positron beam has a small population with higher energies (>150 eV, the maximum retarding potential applied); these particles generate less than 2% of the total luminescence of a ~ 0.1 pA beam on a -5-keV-biased screen.

As expressed in Eq. 1–2 of the main manuscript, measurements of beam current I are needed to make absolute comparisons between positron and electron luminescence. These were taken with the screen connected to ground through a picoammeter (Keithley). Corresponding luminescence measurements for each beam current were taken at an attractive screen bias of several kV. In all four cases (for both species and both phosphors), this yielded a linear relationship betwen L and I; the plots in Fig. 3 show representative values and uncertainties at an attractive screen bias of 5 kV. Based on the slopes of the linear fits, 5-keV positrons produced more luminescence than 5-keV electrons by a factor of 1.42+/-0.08 for ZnS(Ag) and 1.51+/-0.16 for ZnO(Zn). A small additional correction was then applied to the positron current calibration, after gamma measurements indicated that the strength of the positron beam increases by 7–13% when the screen is negatively biased, as compared

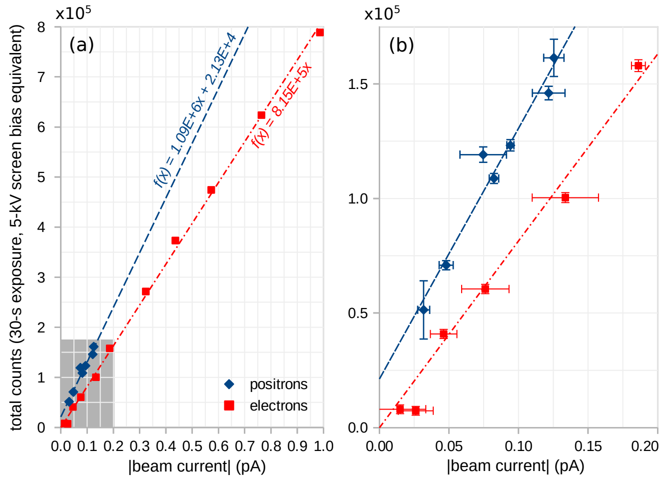

FIG. 3. Luminescence versus beam current magnitude for positrons (blue diamonds) and electrons (red squares) incident on ZnS(Ag). The gray area in panel (a) is shown in greater detail in panel (b). Error bars in (a) are on the order of the symbol size.

to when it is grounded. The final value of $g_+(5\text{ kV})/g_-(5\text{ kV})$ is therefore 1.29+/-0.08 for ZnS(Ag) and 1.37+/-0.15 for ZnO(Zn). These were used to set the relative scaling of the two vertical axes in the plots of $g(V)$ (Fig. 1, 3 of the main manuscript) and to calculate absolute luminescence comparisons (Fig. 4).

For the sake of completeness, we note that all data points in Fig. 3 have been corrected for a slowly varying instrumental offset found in the picoammeter measurements. For electron data points (which were taken on a much faster timescale than the variation), the value of this offset (0.13 pA) was calculated from the data itself; as a result, the linear fit for the electrons goes precisely through the origin. For the positron data points, each of which was taken on a different day, this offset was determined for and subtracted from each current measurement point individually; values ranged from -1.1 to $+0.1$ pA and uncertainties are incorporated into the error bars. After this correction, the linear fit to the positron data points in Fig. 3 remains nontrivially offset from the origin. This reflects mild contamination of the positron beam by low-energy (10s to 100s of eV) secondary electrons from the neon moderator. These do not produce any detectable luminescence from ZnS(Ag) when the phosphor screen is unbiased or biased negatively to attract positrons, but they can be visualized by biasing the screen to large positive voltages (e.g., +5 kV). The resulting luminescence is consistent with a contaminent electron current of $\sim$0.1 pA, which is within the uncertainty of the

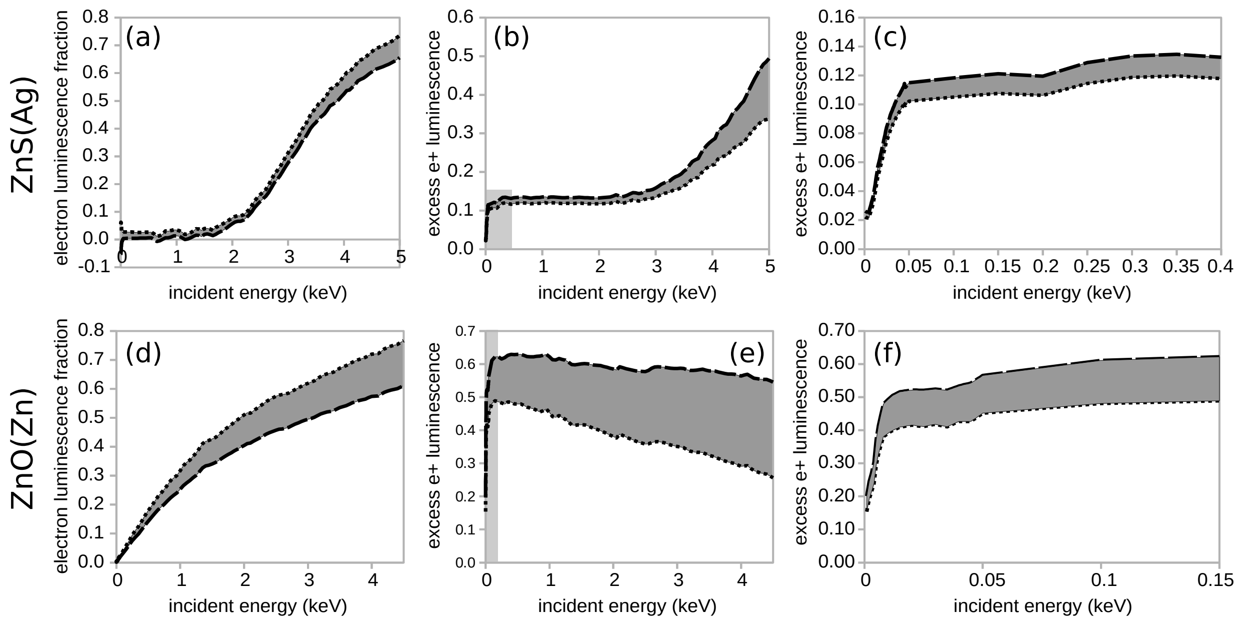

FIG. 4. (a,d) The ratio L_-/L_+ of each phosphor's electron response to its positron response. (b,e) The difference $L_+ - L_-$ between the phosphor's positron and electron responses, normalized to $L_-(5\ \mathrm{kV})$. The gray boxes near the origin in (b,e) indicate the regions shown in greater detail in (c,f).

x-intercept of the linear fit in Fig. 3.

Figure 4 shows several representations of the luminescence data of the two species for each phosphor, each as a function of incident particle energy. In all plots, the shaded region indicates the values that satisfy the data within uncertainties, and the dashed (dotted) lines correspond to the upper (lower) bound on the electron luminescence as a fraction of the positron luminescence. Immediately notable is that for both phosphors, the electron luminescence fraction L_-/L_+ increases monotonically from 0% at the lowest incident energies measured to ∼70% at the highest, and it is still increasing at 5 keV (Fig. 4(a,d)). Or equivalently, $1 - L_-/L_+$ decreases from 100% to about ∼30% and is still decreasing at 5 keV. In the limit of high incident particle energies, the difference between positron-induced and electron-induced luminescence is expected to become negligible compared to the total amount of luminescence produced by either species, consistent with the two previous quantitative comparisons of positron and electron luminescence that we found in the literature [1, 2], both done with higher-energy beams ($\geq$ 30-keV).

[1] K. Gubernator, P. Heckmann, and A. Flammersfeld, Zeitschrift fuer Physik **158**, 268 (1960).

[2] O. I. Meshkov, V. V. Smaluk, D. P. Sukhanov, E. N. Galashov, V. Dorokhov, A. N. Zhuravlev, and V. A. Kiselev, Proceedings of the 10th European Workshop on Beam Diagnostics and Instrumentation for Particle Accelerators , 558 (2011).